Incorporating Patient Breathing Variability into a Stochastic Model of Dose Deposition for Stereotactic Body Radiation Therapy

Sarah E. Geneser[1], Robert M. Kirby[1], Brian Wang[2], Bill Salter[2], and Sarang Joshi[1]

[1] Scientific Computing and Imaging Institute, University of Utah, Salt Lake City, UT, USA
[2] Huntsman Cancer Institute, University of Utah, Salt Lake City, UT, USA
geneser@sci.utah.edu

Abstract. Hypo-fractionated stereotactic body radiation therapy (SBRT) employs precisely-conforming high-level radiation dose delivery to improve tumor control probabilities and sparing of healthy tissue. However, the delivery precision and conformity of SBRT renders dose accumulation particularly susceptible to organ motion, and respiratory-induced motion in the abdomen may result in significant displacement of lesion targets during the breathing cycle. Given the maturity of the technology, sensitivity of dose deposition to respiratory-induced organ motion represents a significant factor in observed discrepancies between predictive treatment plan indicators and clinical patient outcome statistics and one of the major outstanding unsolved problems in SBRT. Techniques intended to compensate for respiratory-induced organ motion have been investigated, but very few have yet reached clinical practice. To improve SBRT, it is necessary to overcome the challenge that uncertainties in dose deposition due to organ motion present. This requires incorporating an accurate prediction of the effects of the random nature of the respiratory process on SBRT dose deposition for improved treatment planning and delivery of SBRT. We introduce a means of characterizing the underlying day-to-day variability of patient breathing and calculate the resulting stochasticity in dose accumulation.

Keywords: stochastic dose deposition modeling, respiratory-induced organ motion, stereotactic body radiation therapy, polynomial chaos, stochastic collocation.

1 Introduction

Hypo-fractionated stereotactic body radiation therapy (SBRT) employs three-dimensional conformal therapy and stereotactic targeting to reduce treatment volumes as well as the number of fractions necessary to deliver extremely large ablative doses and dramatically increase the likelihood of tumor control [1]. The precision and conformity of SBRT-predicted dose to physician-defined tumor target

J.L. Prince, D.L. Pham, and K.J. Myers (Eds.): IPMI 2009, LNCS 5636, pp. 688–700, 2009.
© Springer-Verlag Berlin Heidelberg 2009

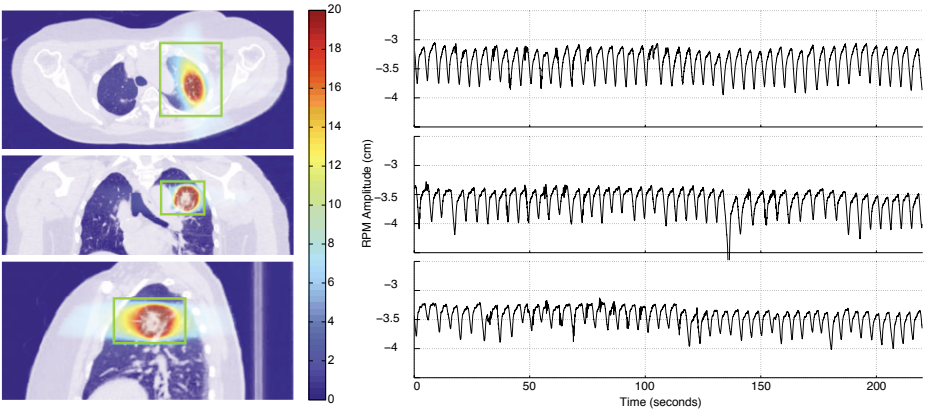

Fig. 1. The static dose plan and Real-time Position Management^{TM}(RPM) traces for a typical SBRT lung cancer patient illustrates the high spatial gradients of target-conforming dose and day-to-day variations in breathing. The static deposited dose (in units of Gray) is color-mapped for the anatomy for axial, sagittal, and coronal views according to the colorbar of the axial view. The RPM breathing traces are recorded for the same patient and time interval on different days.

geometry (evident in the static-dose calculation depicted in Figure Fig. 1) reduce the collateral damage inflicted upon surrounding healthy tissue, particularly in cases where the tumor is stationary during treatment.

State-of-the-art commercial treatment-planning systems are currently capable of calculating accurate dose distributions for only the static case in which the tumor and surrounding tissues are unmoving for the duration of the dose-delivery. However, respiratory-induced organ motion results in significant movement of lesion targets during the breathing cycle [2,3] as evidenced in Fig. 2. Because SBRT is particularly susceptible to motion of the targeted tumor, patient respiration can lead to significant dose-delivery errors. Several studies have investigated the dosimetric consequences of respiratory-induced tissue motion on SBRT and found variations between planned and delivered dose distributions as significant as 20% [4].

Controlling patient breathing during treatment and restricting beam-on times to windows of low variation in patient anatomy are two means of minimizing the variability in dose deposition due to respiratory-induced motion. A number of methods exist to reduce dose variation (e.g., respiratory gating [5], breath-hold [6], and coached breathing [7]). However, such techniques have drawbacks and none are appropriate for all patients as they either induce an unacceptable level of patient discomfort (e.g., due to their compromised respiratory function, many lung cancer patients cannot tolerate breath-hold methods), significantly increase the treatment time (e.g., during respiratory-gated treatment, the beam is only on for a small fraction of the treatment period, necessitating a much extended treatment time), or may be impractical (e.g., in the case of coached

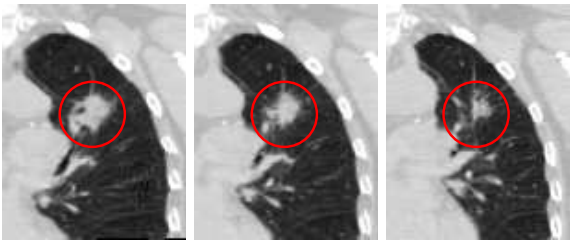

Fig. 2. Respiratory-induced organ motion can cause significant movements of the tumor. These coronal slices represent anatomy corresponding to three breathing amplitudes. Note the displacement of the tumor within the stationary red outline.

breathing, some patients are not trainable). While some radiation oncologists employ these methods, most instead design a treatment based on simple mechanisms, e.g., the inclusion of a border or "margin" around the defined target volume. This technique is widely employed to limit the impact of motion on dose deposition; however, it ensures a complete treatment of the target at the expense of irradiating adjacent healthy tissues. Indeed, breathing motion remains one of the major obstacles to reducing the irradiation volume while maintaining a high probability of tumor control.

Patients may exhibit markedly different breathing patterns between treatment fractions. The fundamentally random nature of respiration can result in delivered doses that significantly vary from treatment to treatment. Failure to accommodate for patient-specific breathing stochasticity can result in under-dosing of the target and deposition of dangerous dose levels to surrounding healthy tissue. When limiting variability of patient organ-motion during treatment is impossible or unreasonable, it is essential to incorporate an accurate prediction of the effects of the stochastic respiratory process on SBRT dose deposition for safe and effective treatment-planning and delivery of SBRT. Though several groups have worked to develop accurate models that incorporate the effect of respiratory-induced organ motion on dose deposition [8], we know of no studies that incorporate a patient-specific stochastic model of breathing variability into dose calculations and no computational tools yet exist to accomplish this goal. The aim of this work is to compute the stochasticity in dose accumulation for SBRT treated lesions resulting from stochastic organ motion induced by variations in day-to-day patient breathing patterns.

We begin by developing a framework for modeling patient specific breathing as a stochastic process. To quantify the stochasticity in patient breathing patterns we parametrize the recorded patient breathing traces and model the resulting breathing parameters as random variables. Once we estimate the underlying distributions of the random variables, we incorporate our stochastic breathing model into a calculation of the stochastic dose that accounts for variations in organ motion during treatment. We may then calculate any pertinent statistics of the stochastic dose.

2 Methods

To account for stochastic respiratory-induced tumor motion, we must first accurately quantify the impact of organ motion on dose deposition over the course of a treatment. This necessitates an accurate patient specific anatomical model over the course of the treatment and the ability to calculate the dose deposition at each anatomical configuration observed during treatment. Commercially available respiratory-correlated CT (RCCT) [9,10] tools provide a means of visualizing four-dimensional organ motion, and clinicians currently rely on the detailed images produced from such scans to generate the contours of targeted volumes to be irradiated. However, tumor volumes and margins for treatment-planning are generated from images obtained on a single day, and fail to consider the stochastic nature of breathing. Using deformable image registration techniques, the anatomical data from all different anatomical conformations during breathing can be mapped onto a common geometry. The mapping can further be used to compute the dose deposition resulting from any observed or simulated respiratory-induced organ motion during treatment [11,12]. By analyzing patient respiratory patterns, we generate a stochastic model of breathing variability. We then incorporate this into an estimate of the stochasticity in total deposited energy resulting from a distribution of breathing-induced organ motion.

2.1 Incorporating Organ Motion into Dose Calculation

To calculate the effect of respiratory-induced organ motion on dose deposition, we first build an explicit model of tissue deformation from anatomical patient images that depict respiratory-induced organ motion. Our motion model and subsequent dose calculations rely on the well-justified and widely accepted assumption that the position of the anatomy is a function of breathing pattern (measured by some external signal e.g., Varian's Real-Time Position Management (RPM) system). Several groups have investigated the correlation between external and internal motion markers [13,14] and reported high correlation between them.

From the patient images, it is essential to construct a deformation field, $h(x, a(t))$, which maps each spatial point, x, in a base image according to the deformation of the anatomy as a function of breathing amplitude. Generating deformation fields that model organ motion is a well-studied problem and several groups have developed techniques that produce accurate deformation fields from artifact-free CT images [15,16]. We employ these well-established image registration methods to construct an amplitude-indexed high-dimensional transformation that maps sequential CT images to a base anatomy on which we calculate dose.

The dynamic dose deposition, D, accounting for the organ motion during a treatment is integrated over the treatment time interval $[0, T]$ as follows:

$$D = \int_0^T d(h(x, a(t)), a(t))dt,$$

where $d(h(x, a(t)), a(t))$ is the static dose corresponding to the amplitude of the breathing signal during treatment, $a(t)$, and mapped to the base image according to the deformation field $h(x, a(t))$. A change of variables yields the total deposited dose over a treatment period as an integral over the amplitudes,

$$D = \int_{min(a)}^{max(a)} d(h(x, a), a) w(a) da, \tag{1}$$

where $w(a)$ is the time density of the breathing amplitudes. Given a set of amplitude-binned CT images and a model of the organ deformation as described above, we estimate delivered dose by discretizing Eq. 1 to obtain a weighted sum of amplitude-indexed dose images as follows:

$$D = \sum_{i=0}^{N} w_i d(h(a_i), a_i), \quad w_i = \int_{a_i - \delta a}^{a_i + \delta a} f(x) dx,$$

where $f(x)$ is a quantification of the relative density of breathing amplitudes over treatment time and $\delta a = \frac{1}{2}(a_{i+1} - a_i)$ is the size of the amplitude discretization. The term $d(h(a_i), a_i)$ corresponds to the calculated dose deposited at a particular breathing amplitude, a_i, and the weights, w_i, account for the relative amount of time the tissue spends at the anatomical configuration corresponding to the amplitude, a_i, during the treatment period.

It is important to stress that the model of dose distribution, D, as presented above accounts only for the respiratory-induced organ motion observed during a single treatment. As such, it includes none of the observed day-to-day variability in a patient's breathing motion. For D to give insight to the effects of day-to-day variability, one must incorporate a model of patient breathing variability as the input to the dose deposition calculation. In the following sections, we provide the framework to determine the stochasticity in daily breathing patterns and to apply our stochastic model to determine the resulting variations in dose distribution.

2.2 Parametrization of Breathing Amplitude Density

The extent of breathing variability differs from patient to patient, necessitating patient-specific models of breathing variability to generate accurate predictions of dose deposition resulting from variations in day-to-day breathing patterns. In particular, because the time density of breathing amplitudes is sufficient to calculate dose distribution, we need only determine the day-to-day variations in amplitude density as a function of time, which we model as a stochastic process.

To parametrize and estimate the amplitude density of each patient breathing trace, we fit a Gaussian Mixture Model (GMM) to the set of recorded amplitudes from each patient breathing trace [17]. Given the parameters of the individual breathing trace amplitudes, we can then analyze the characteristics of variability for the patients and build a model to capture the patient-specific stochasticity in breathing amplitudes.

GMMs provide a means of parametrizing the probability density of a random process and thus the amplitude density of RPM breathing traces. Such models are convex combinations of M Gaussian probability distributions as follows,

$$m(x, p_i, \mu_i, \sigma_i) = \sum_{i=1}^{M} p_i \frac{1}{\sigma_i \sqrt{2\pi}} e^{\frac{-(x-\mu_i)^2}{2\sigma_i^2}} \tag{2}$$

where μ_i and σ_i are the mean and standard deviation of the i^{th} Gaussian distribution and p_i are positive weighting factors that sum to one. We fit these parameters to patient RPM breathing traces using the well-known Expectation Maximization (EM) algorithm [18,17]. Because patients pause at inhale and exhale and the amplitudes for both are typically consistent over time, one observes peaks in the amplitude density function at both locations. As a consequence, one might conjecture that a two Gaussian mixture model is appropriate for estimating and parametrizing the amplitude density of RPM breathing traces.

2.3 Model of Breathing Variability

In order to quantify the daily variability in the patient specific dose accumulation, we first characterize the variability in the patient's breathing patterns. Because we have parametrized the estimates of the daily amplitude density of patient breathing, we require a formulation of the variation of these parameters from day-to-day. To accomplish this, we performed principal component analysis (PCA) [19] on the model parameters. A two-Gaussian mixture model has five parameters. Using PCA, we identify the components of greatest variation in the GMM parameters.

We formulate the stochasticity in the GMM model parameters as a function of independent and uncorrelated Gaussian random variables, $\boldsymbol{\xi} = (\xi_1, \ldots, \xi_P)$ where P is the number of principal components necessary to accurately capture the breathing variability. This analysis allows us to formulate the variability as a stochastic function of the Gaussian distributed principal components.

2.4 Variations in Dose

Given a model of patient-specific variability in respiratory-induced organ motion and dose calculation, we can now compute statistics of the deposited dose from a single fraction. With the variation in the GMM parameters expressed in terms of a P-dimensional random variable, $\boldsymbol{\xi}$, we incorporate the stochastic model into a statistical characterization of the dose distribution, D, resulting from variations in respiratory-induced organ motion. Because the dose distribution is a direct consequence of anatomical configuration, the dose is expressed as a function of $\boldsymbol{\xi}$, and we denote the dose as $D(\boldsymbol{\xi})$. In our study, we are interested in computing statistics (e.g., mean and variance) on the stochastic dose deposition, $D(\boldsymbol{\xi})$. Based upon these quantities, we can assess the impact of respiratory-induced organ motion variability on generation and interpretation of predicted SBRT dose distributions.

Monte Carlo (MC) techniques are an obvious first choice for computing statistics of a random field like $D(\boldsymbol{\xi})$. Such an approach requires sampling the stochastic GMM parameter space to obtain dose deposition for each treatment realization. However, because Monte Carlo requires a very large number of samples for sufficient convergence of computed statistics, and each dose calculation requires sufficiently long computing time, the inordinate time necessary to calculate accurate statistics using Monte Carlo renders the approach infeasible, especially for clinical use.

2.5 Generalized Polynomial Chaos-Stochastic Collocation

We employ the generalized polynomial chaos-stochastic collocation (gPC-SC) method [20,21] as a computationally efficient and easily implemented alternative to MC sampling. Unlike traditional MC, in which very large numbers of collocation points are required to compute accurate statistics, only a limited number of samples are necessary. The gPC-SC approach requires that the stochastic aspects of the system be mathematically characterizable stochastic processes to take advantage of quadrature rules to integrate the stochastic process of interest over the appropriate domain. Like MC methods, gPC-SC is a sampling method in that it does not require derivation of the stochastic approximating system. In contrast to MC, where the deterministic system must be solved at a very large set of randomly chosen sample values of the stochastic input process, gPC-SC exploits assumptions concerning the mathematical nature of the stochastic system of interest to minimize the number of samples necessary for accurate statistics. Under assumptions of smoothness of the system with respect to inputs, which in this case equate to the recognition that the dose distributions vary smoothly as a function of the breathing patterns, we gain exponential convergence in the statistical accuracy as a function of the number of dose distribution forward simulations we compute. This process yields a sequence of solutions for a small and far more computationally tractable number of specific realizations of the stochastic field. These solutions are then used to obtain highly accurate estimates of the mean, variance, and higher statistical moments of the system.

The generalized polynomial chaos (gPC) method provides a means of representing stochastic processes as a linear combination of orthogonal stochastic polynomials [22]. In our case, the GMM parameters are Gaussian distributed, and are represented exactly by two Hermite polynomials. Because dose calculation is a non-linear process with respect to the GMM parameters and patient anatomy, the distribution of dose will be non-Gaussian. Stochastic processes with arbitrary or non-Gaussian distributions are represented using weighted sums of Hermite polynomials as follows: $\boldsymbol{\xi}(\omega) = \sum_{i=0}^{N} \alpha_i H_i(\omega)$, where ω is a random variable and α_i is a weight obtained by projecting the stochastic process onto the i^{th} Hermite polynomial.

The stochastic collocation approach consists of selecting a collection of points at which to sample the random field and corresponding weights that account for the underlying stochastic characteristics of the system. Each collocation point, $\boldsymbol{\xi}_i$, represents a particular breathing amplitude density for the duration of a

treatment selected from the set of likely breathing patterns. We compute the dose deposition for each collocation realization, $D(\boldsymbol{\xi}_i)$, by the method described in Sec. 2.1.

For Gaussian distributed random variables, ψ, of mean zero and unit variance, the collocation points, ψ_i, are the roots of the Hermite polynomials and the weights, c_i, are given by $c_i = \frac{2^{n-1} n! \sqrt{\pi}}{n^2 (H_{n-1}(\psi_i))^2)}$. Though polynomial roots can be approximated using a root-finding method like Newton's method, it is faster to use the Golub-Welsch algorithm [23] in the case of Hermite polynomials [24]. We obtain the Hermite roots by calculating the eigenvalues of the Jacobi matrix, J, composed of the recurrence relation coefficients of the Hermite polynomials, and the weights are equivalent to the first component of the normalized eigenvectors of the Jacobi matrix J [24]. To accommodate Gaussian random variables, $\boldsymbol{\xi}$, of arbitrary mean, μ, and variance, σ^2, we map the collocation points as follows: $\boldsymbol{\xi}_i = \sigma\psi_i + \mu$. The collocation weights and points can be extended to multiple stochastic dimensions using tensor products for lower dimensions or the Smolyak construction [20,21] for higher dimensions.

For each collocation point, $\boldsymbol{\xi}_i$, representing a particular breathing amplitude density for the duration of a treatment we calculate the corresponding dose deposition, $D(\boldsymbol{\xi}_i)$. The mean and variance of the deposited dose are calculated using the forward dose computations and the collocation weights as follows:

$$\mathbb{E}[D(\boldsymbol{\xi})] \approx \sum_{i=0}^{N} c_i D(\xi_i) \quad \text{and} \quad \mathbb{E}[(D(\boldsymbol{\xi}) - \mathbb{E}[D(\boldsymbol{\xi})])^2] \approx \sum_{i=0}^{N} c_i (D(\xi_i) - \mu(D(\boldsymbol{\xi})))^2.$$

3 Results

In this section we present results for a lung cancer patient undergoing stereotactic body radiation treatment (SBRT) of 60 Gy total dose over 3 fractions at the Department of Radiation Oncology at the Huntsman Cancer Institute. The static dose plan for the patient is depicted for axial, sagittal, and coronal CT slices in Fig. 1 along with three representative RPM traces recorded for the patient on different days.

We collected 4DCT images on a 16-slice large bore LightSpeed RT CT scanner (Ge Health Care, Waukesha, WI) using the 4D RCCT [9,10] scan protocol described below. Scans at each couch position were continuously acquired in the axial cine mode for a period of time equal to the maximum breathing cycle plus one second with a 0.5 second per revolution gantry rotation speed and slice thickness of 1.25 mm at 120 kVp and 436 mA. A total of roughly 2900 CT slices were acquired at 187 couch positions. The patient's chest amplitude was continuously recorded during CT acquisition using Varian's RPM system. A total of six RPM traces were recorded during CT imaging on different treatment days and subsequently analyzed to determine the variability in patient breathing behavior.

To generate a set of amplitude indexed three-dimensional images from the CT slices, we first generated two amplitude binned images near the minimum and

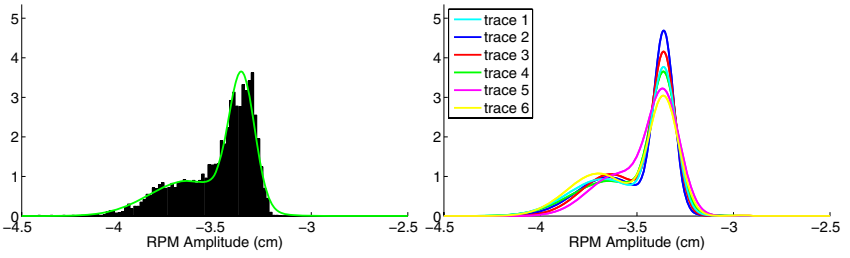

Fig. 3. The Gaussian mixture model provides an estimation of amplitude densities of the RPM breathing traces. The GMM fit for a single RPM trace overlays the histogram of amplitudes in the left image. The day-to-day variations in amplitude density of the RPM breathing traces recorded on several different days are evident on the right image.

maximum of the RPM signal. We then performed deformable image registration using the method of Keall et al., [12] to obtain a deformation field and linearly interpolated along that field to produce anatomical images corresponding to any chosen amplitude between the minimum and maximum. In a similar manner, we construct dose depositions for arbitrary amplitude by applying the deformation field to the base image dose deposition calculated using the BrainScan v5.31 treatment-planning system (BrainLAB AG, Munchen, Germany).

Figure 3 depicts the normalized histogram of and GMM fit to the amplitudes of the middle RPM trace depicted in Fig. 1. By visually comparing the GMM fit with the histogram of the breathing amplitudes, it is evident that the model provides an appropriate fit for the data. The six GMM estimations of amplitude density recorded for the same patient on different days depicted in the right image of Fig. 3 clearly illustrate the day-to-day variability in breathing amplitude density.

Examination of the eigenvalues corresponding to variation in the parameters depicted in the right image of Fig. 4 suggests that only three PCA components

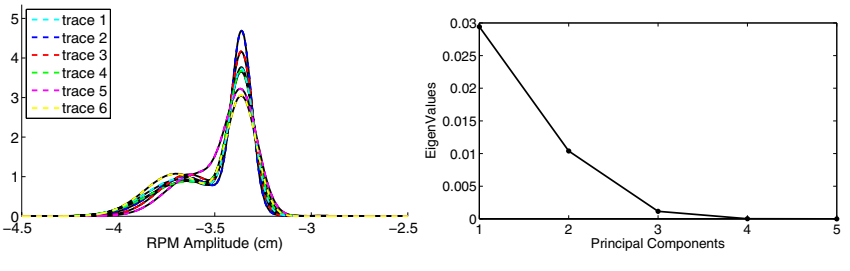

Fig. 4. The PCA reduction of the Gaussian mixture models gives very close reconstructions to the original mixture models with only three independent and uncorrelated eigenvectors. The eigenvalues of the principal components of the Gaussian Mixture Model parameters are negligible for the fourth and fifth components, confirming that only three are necessary to accurately capture the variation observed in the breathing traces.

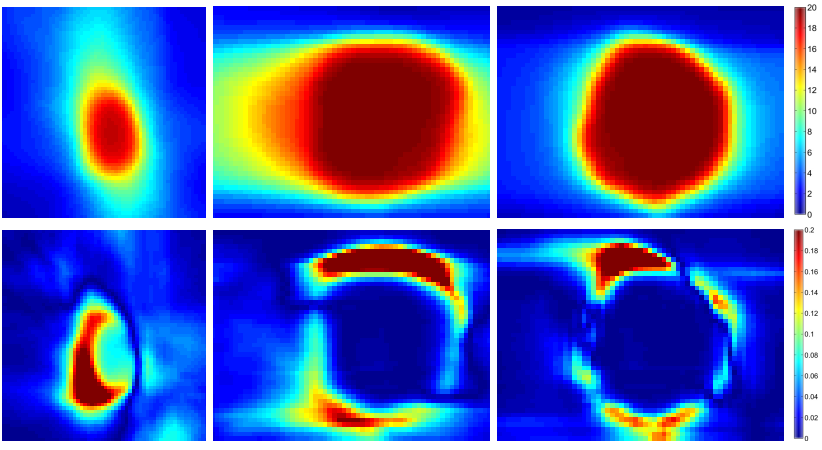

Fig. 5. The average (top row) and standard deviation (bottom row) of stochastic dose deposition (in Gray) is depicted in axial, sagittal, and coronal views, respectively. The regions of interest correspond to those in Fig. 1.

are necessary to accurately capture the variability in breathing. This enables a reduction of the stochastiSc dimensionality from five to three with at most, a 1.46×10^{-3} root mean squared error between the original and reduced GMMs. For visual comparison, the reconstruction of the GMM models for the six RPM breathing traces is depicted in left image of Fig. 4. The close correspondence between the original fitted GMMs and the GMMs reconstructed from a reduced dimensionality via PCA allows significant reduction in the complexity of the stochastic system owing to the correspondingly reduced dimensionality of the stochastic space.

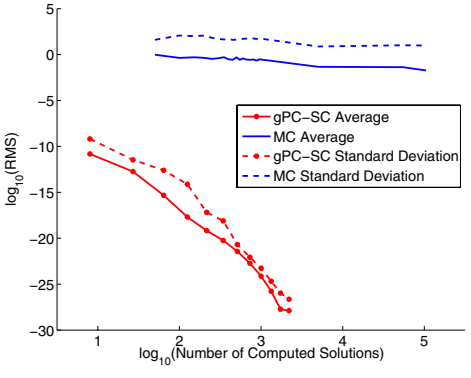

Fig. 6. The convergence rates for MC and gPC-SC methods as used to compute average and standard deviation of the deposited dose.

Figure 5 depicts the average and standard deviations of deposited dose over a single treatment for axial, sagittal, and coronal views. A comparison of the average dose depositions to the static-dose deposition calculation in Fig. 1 shows little difference. However, examination of the standard deviation in dose shows non-trivial high values (greater than 0.2 Gray) occurring near the boundaries of the lesion. We observed that large standard deviations in dose often correspond to regions of high dose gradient that undergo large respiratory-induced organ deformation. Such areas are significant because they indicate regions in which

the planned dose may differ significantly from the actual deposition during treatment and are likely candidates for over- or under-dosing.

To validate our approach, we present in Fig. 6 the convergence in gPC-SC and traditional MC dose statistics for the patient case depicted in Fig. 5. The convergence data depicted is the root mean squared (RMS) difference between the current and final number of forward solutions for the average and standard deviation of dose calculations. It is clear that with only $2,744$ realizations the gPC-SC method has reached greater convergence than the MC method with $155,000$ forward dose solutions. Thus, for this particular model, gPC-SC exhibits significantly faster convergence than MC.

4 Discussion

The goal of this study was to develop a framework for quantifying the variability in respiratory-induced organ motion and incorporate that stochastic model into the calculation of dose deposition for SBRT treatment-planning. In contrast to Monte Carlo methods which are clinically infeasible because they require days or even weeks to compute accurate dose deposition statistics, the efficiency of the proposed approach enables physicians to perform statistical studies of dose response to breathing induced organ motion on a clinically realistic time scale. Statistical dose computations are particularly useful in planning because they allow physicians to identify and avoid dose plans in which high standard deviations in dose coincide with radiation sensitive tissues e.g., the spinal cord. We propose that accurate statistical models of predicted dose deposition resulting from organ motion will enable physicians to better assess the impact of SBRT dose plans on normal tissue and tumor lesions.

Acknowledgements. The authors would like to acknowledge the computational support and resources provided by the Scientific Computing and Imaging Institute. This work was funded by a University of Utah Synergy Grant No. 51003269. Support for the acquisition of the data used within the simulation studies came from the Huntsman Cancer Institute. The authors would also like to thank Jacob Hinkle for providing the amplitude-binned images used in this work.

References

1. Timmerman, R., Forster, K., Chinsoo Cho, L.: Extracranial stereotactic radiation delivery. Semin. Radiat. Oncol. 15, 202–207 (2005)
2. Lujan, A., Larsen, E., Balter, J., Ten Haken, R.: A method for incorporating organ motion due to breathing into 3D dose calculations. Med. Phys. 26, 715–720 (2003)
3. Brandner, E., Wu, A., Chen, H., Heron, D., Kalnicki, S., Komanduri, K., Gerszten, K., Burton, S., Ahmed, I., Shou, Z.: Abdominal organ motion measured using 4D CT. Int. J. Radiat. Oncol. Biol. Phys. 65, 554–560 (2006)

4. Wu, Q., Thongphiew, D., Wang, Z., Chankong, V., Yin, F.: The impact of respiratory motion and treatment technique on stereotactic body radiation therapy for liver cancer. Med. Phys. 35(4), 1440–1451 (2008)
5. Keall, P., Kini, V., Vedam, S., Mohan, R.: Potential radiotherapy improvements with respiratory gating. Australas. Phys. Eng. Sci. Med. 25, 1–6 (2005)
6. Hanley, J., Debois, M., Raben, A., et al.: Deep inspiration breath-hold technique for lung tumors: The potential value of target immobilization and reduced lung density in dose escalation. Int. J. Radiat. Oncol. Biol. Phys. 36(1), 188 (1996)
7. Neicu, T., Berbeco, R., Wolfgang, J., Jiang, S.: Synchonized moving aperture radiation therapy (SMART): Improvement of breathing pattern reproducibility using respiratory coaching. Phys. Med. Biol. 51, 617–636 (2006)
8. Boldea, V., Sharp, G., Jiang, S., Sarrut, D.: 4D-CT lung motion estimation with deformable registration: Quantification of motion nonlinearity and hysteresis. Med. Phys. 35(3), 1008–1018 (2008)
9. Ford, E., Mageras, G., Yorke, E., Ling, C.: Respiration-correlated spiral ct: A method of measuring respiratory-induced anatomic motion for radiation treatment planning. Med. Phys. 30, 88–97 (2003)
10. Vedam, S., Keall, P., Kini, V., Mostafavi, H., Shukla, H., Mohan, R.: Acquiring a four-dimensional computed tomography dataset using an external respiratory signal. Phys. Med. Biol. 48(1), 45–62 (2003)
11. Foskey, M., Davis, B., Goyal, L., Chang, S., Chaney, E., Strehl, N., Tomei, S., Rosenman, J., Joshi, S.: Large deformation three-dimensional image registration in image-guided radiation therapy. Phys. Med. Biol. 50, 5869–5892 (2005)
12. Keall, P., Joshi, S., Vedam, S., Siebers, J., Kini, V., Mohan, R.: Four-dimensional radiotherapy planning for DMLC-based respiratory motion tracking. Med. Phys. 32, 942–951 (2005)
13. Beddar, A., Kainz, K., Briere, T., Tsunashima, Y., Pan, T., Prado, K., Mohan, R., Gillin, M., Krishnan, S.: Correlation between internal fiducial tumor motion and external marker motion for liver tumors imaged with 4D-CT. Int. J. Radiat. Oncol. Biol. Phys. 67(2), 630–638 (2007)
14. Ionascu, D., Jiang, S., Nishloka, S., Shirato, H., Berbeco, R.: Internal-external correlation investigations of respiratory induced motion of lung tumors. Med. Phys. 34(10), 3893–3903 (2007)
15. Pevsner, A., Davis, B., Joshi, S., et al.: Evaluation of an automated deformable image matching method for quantifying lung motion in respiration-correlated CT images. Med. Phys. 33(2), 369–376 (2006)
16. Wijesooriya, K., Weiss, E., Dill, V., Dong, L., Mohan, R., Joshi, S.: Quantifying the accuracy of automated structure segmentation in 4D CT images using a deformable image registration algorithm. Med. Phys. 35(4), 1251–1260 (2008)
17. McLachlan, G., Peel, D.: Finite Mixture Models. John Wiley & Sons, Inc., New York (2000)
18. Dempster, A., Laird, N., Rubin, D.: Maximum likelihood from incomplete data via the EM algorithm. J. Roy. Stat. Soc. B. Met. 39(1), 1–38 (1977)
19. Pearson, K.: On lines and planes of closest fit to systems of points in space. Philos. Mag. 2(6), 559–572 (1901)
20. Xiu, D., Hesthaven, J.: High-order collocation methods for differential equations with random inputs. SIAM Journal on Scientific Computing 27(3), 1118–1139 (2005)
21. Xiu, D.: Efficient collocational approach for parametric uncertainty analysis. Comm. Comput. Phys. 2(2), 293–309 (2007)

22. Xiu, D., Karniadakis, G.: The Wiener-Askey polynomial chaos for stochastic differential equations. SIAM J. Sci. Comput. 24, 619–644 (2002)
23. Golub, G., Welsh, J.: Calculation of Gauss quadrature rules. Math. Comput. 10, A1–A10 (1969)
24. Press, W., Teukolsky, S., Vetterling, W., Flannery, B.: Gaussian Quadratures and Orthogonal Polynomials. In: Numerical recipes in C: The art of scientific computing, 2nd edn., pp. 147–161. Cambridge University Press, New York (1992)